Supporting information

pyro-photo-electric catalysis and photoelectrochemical measurements

To evaluate how the interface affects pyro-photo-electrical catalysis performance, the process is studied in the three-electrode system with a 0.5 M Na_2SO_4 electrolyte solution at a scan rate of 0.1 V s^{-1}. In the three-electrode system, the temperature change (ΔT = 20℃-50 ℃) is achieved by water bath method, two different temperature baths of 20°C and 50°C are prepared for accelerating the heating and cooling the electrolyte. Fig. S4 gives an ideal temperature change curve, the scanning rate of the electrochemical workstation is determined by the rate of temperature change set by the curve. The Light conditions achieved with a 300 W xenon lamp equipped with an AM 1.5 G filter (100 mW·cm^{-2}). The Platinum wire is used as an auxiliary electrode, Ag/AgCl is used as a reference electrode, FTO with a coating area of approximately 1 cm^2 is used as the working electrode. The mechanism diagram of the catalysis process and the energy band structure diagram of heterojunctions are shown in Fig. S5. The relationship between potential and reversible hydrogen electrode (RHE) is calculated by Nernst equation (1):[1]

$$E_{RHE} = E_{Ag/AgCl} + 0.0591\ pH + 0.1976\ V \quad (1)$$

ABPE is calculated by equation (2). Where J means photocurrent density (mA/cm^2), V_{RHE} is the correlation of potential and RHE, and incident light irradiance (mW/cm^2) is expressed by Plight.[2]

$$ABPE = \frac{J_{Ph}(1.23 - V_{RHE})}{P_{light}} \quad (2)$$

The IPCE of samples can be directly characterized by equation (3). Where λ means incident light wavelength (nm). P_{light} indicates the incident monochromatic light intensity (mW/cm^2), and λ represents wavelength (nm).[3]

$$IPCE = \frac{1240J}{\lambda P light} \quad (3)$$

V_{fb}, N_d and W_{dep} are calculated by the equation (4-6). Where C means the space charge capacitance(1.602×10^{-19} C), K_B represents Boltzmann constant (1.38×10^{-23} J/K), T indicates Kelvin temperature, ε and ε_0 are the relative permittivities (8.834×10^{-12} F/m) and the permittivity of vacuum(300) of CdS, e represents elementary charge and A is coated electrode area, the bias voltage applied to the electrodes is expressed by

V. [4-6]

$$1/c^2 = \frac{2(V - V_{fb} - K_B T/e)}{\varepsilon\varepsilon_0 e A^2 N_d} \quad (4)$$

$$N_d = \frac{2}{\varepsilon\varepsilon_0 e}\left[\frac{d(\frac{1}{c^2})}{d_V}\right]^{-1} \quad (5)$$

$$W_{dep} = \sqrt{\frac{2\varepsilon\varepsilon_0(V - V_{fb})}{qN_d}} \quad (6)$$

The η_{bulk} and $\eta_{surface}$ of the working electrodes are computed according to the equations below:[7]

$$J_{H_2O} = J_{abs} \times \eta_{bulk} \times \eta_{surface} \quad (7)$$

J_{H_2O} stands for photocurrent density, and J_{abs} refers to photon absorption represented by current density (100 % photocurrent of APCE is assumed). After adding 0.25 M Na_2SO_3 as the hole scavenger in 0.5 M Na_2SO_4, surface recombination of carriers is inhibited, and $\eta_{surface}$ can be considered for 100 %. Therefore, in the case of hole scavenger addition, the photocurrent density is decided by equation (8).[2]

$$J_{Na_2SO_3} = J_{abs} \times \eta_{bulk} \quad (8)$$

So, the η_{bulk} *and* $\eta_{surface}$ *are calculated by* equations (9) and (10)：

$$\eta_{bulk} = J_{Na_2SO_3}/J_{abs} \quad (9)$$

$$\eta_{surface} = J_{H_2O}/J_{Na_2SO_3} \quad (10)$$

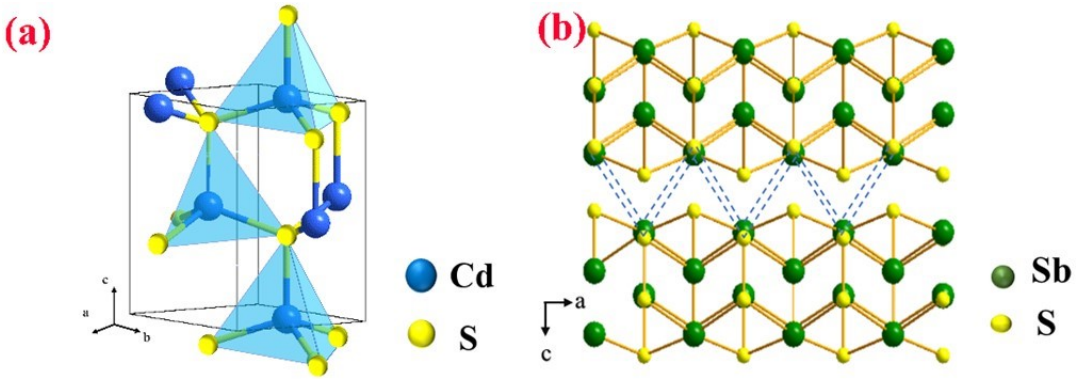

Fig. S1 The asymmetric crystal structure of CdS(a) and Sb_2S_3(b)

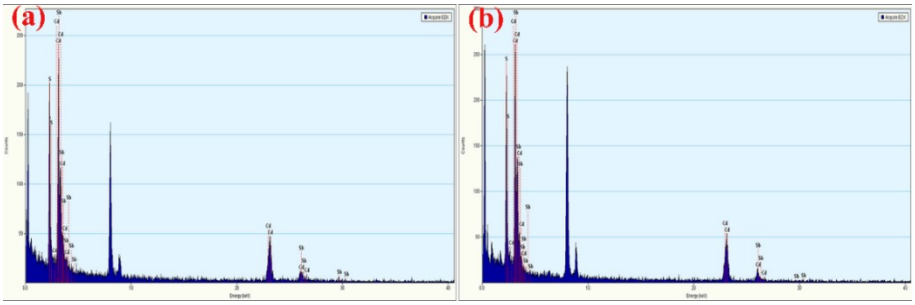

Fig. S2 EDS image of H-CdS/Sb_2S_3(a), and I-CdS/Sb_2S_3(b)

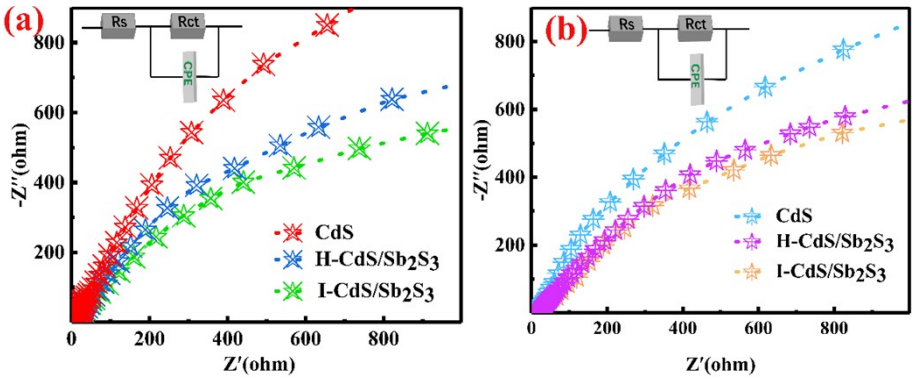

Fig.S3 EIS of different photoanode samples under the photoelectric catalysis (a), pyro-photo-electric catalysis(b)

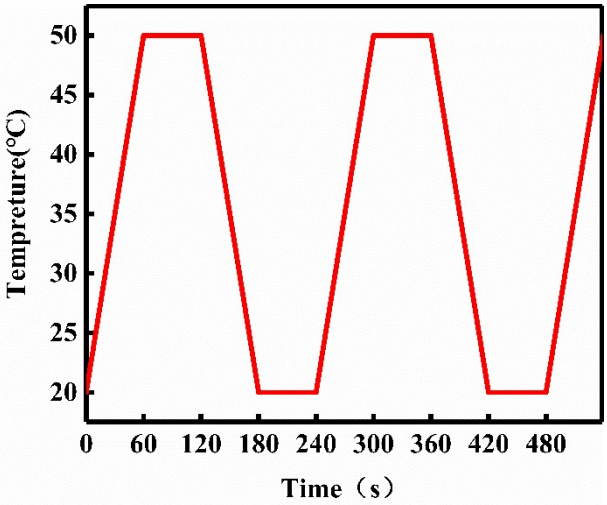

Fig.S4 The ideal temperature curve for cold-hot thermal cycles

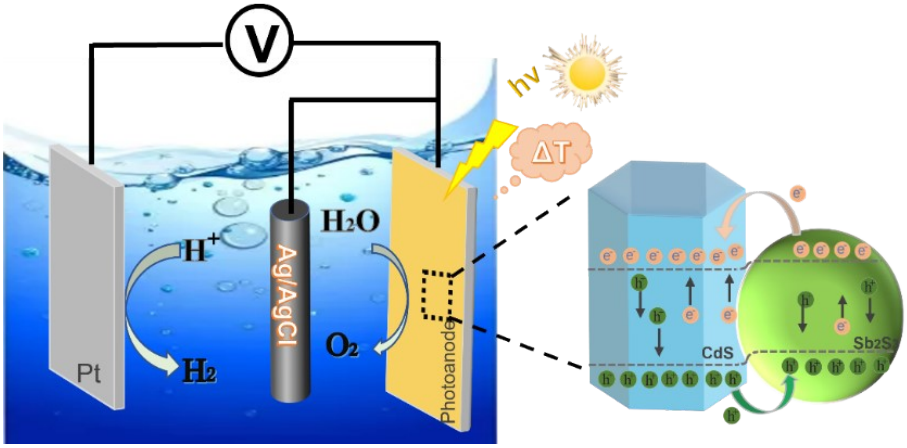

Fig. S5 Mechanism diagram of CdS/Sb_2S_3 heterojunctions

Tab. S1 Flat band potential (V_{fb}) and donor density (N_d) of electrodes deduced from Mott-Schottky

Condition / Sample	Light		Light+△T	
	V_{fb} (V vs RHE)	N_d (cm^{-3})	V_{fb} (V vs RHE)	N_d (cm^{-3})
CdS	0.29	9.20×10^{15}	0.24	8.16×10^{16}
H-CdS/Sb_2S_3	0.16	4.70×10^{16}	-0.21	5.52×10^{17}
I-CdS/Sb_2S_3	0.10	2.04×10^{17}	-0.34	8.85×10^{17}

Tab. S2 W_{dep} of electrodes deduced from Mott-Schottky

Condition / Sample	Light	Light+△T
CdS	2.23×10^{-3}nm	6.36×10^{-4} nm
H-CdS/Sb_2S_3	8.69×10^{-4} nm	2.94×10^{-4} nm
I-CdS/Sb_2S_3	4.28×10^{-4} nm	2.43×10^{-4} nm

References

1 Z. Yang, C. Zhang, G. Zeng, X. Tan, D. Huang, W. Zhou, K. Nie, State-of-the-art progress in the rational design of layered double hydroxide based photocatalysts for photocatalytic and photoelectrochemical H_2/O_2 production, *Coordin. Chem. Rev.*, 2021, 446, 214103.

2 T. Li, Z. Liu, Y. Meng, Two-dimensional ultra-thin nanosheets optimize the surface reaction dynamics and photo/pyro-generated carrier transfer of $NaNbO_3$ for an efficient pyro-photo-electric catalytic system, *Sustain. Energ. Fuels.*, 2022, **6**, 4227-4239.

3 Z. Hao, M. Ruan, Z. Guo, W. Yan, X. Wu, Z. Liu, The synergistic role of the photosensitivity effect and extended space charge region in an inorganic-organic WO_3/PANI photoanode for efficient PEC water splitting, *Sustain. Energ. Fuels.*, 2021, **5**, 2893-2906.

4 H. Chai, P. Wang, T. Wang, L. Gao, F. Li, J. Jin, Surface reconstruction of cobalt species on amorphous cobalt silicate-coated fluorine-doped hematite for efficient photoelectrochemical water oxidation, *ACS Appl. Mater. Inter.*, 2021, **13**, 47572-47580.

5 Wang P, Fu Y, Yu B, Zhao Y, Xing L, Xue X. Realizing room-temperature self-powered ethanol sensing of ZnO nanowire arrays by combining their piezoelectric, photoelectric and gas sensing characteristics, *J. Mater. Chem. A*, 2015, **3**, 3529-3535.

6 X. Yin, X. Yang, W. Qiu, K. Wang, W. Li, Y. Liu, J. Li, Boosting the photoelectrochemical performance of $BiVO_4$ photoanodes by modulating bulk and interfacial charge transfer, *ACS Appl. Electron. Mater.*, 2021, **3**, 1896-1903.

7 M. Radecka, M. Rekas, A. Trenczek-Zajac, K. Zakrzewska., Importance of the band gap energy and flat band potential for application of modified TiO_2 photoanodes in water photolysis, *J. Power Sources*, 2008, **181**, 46-55.